

## $\Sigma^-$ Capture in Deuterium\*†

DONALD E. NEVILLE‡§

*The Enrico Fermi Institute for Nuclear Studies and the Department of Physics,  
The University of Chicago, Chicago, Illinois*

(Received 22 October 1962)

Transition rates for the final states  $\Sigma^0+n+n$  and  $\Lambda+n+n$  are calculated in impulse approximation for  $\Sigma^-d$  capture from rest, taking into account the  ${}^1S_0$   $n$ - $n$  attraction and the tensor term in the  $\Sigma^-p \rightarrow \Lambda n$  transition amplitude. Using the  $\Sigma^-p \rightarrow \Sigma^0 n$  and  $\Sigma^-p \rightarrow \Lambda n$  amplitudes calculated for global symmetry by de Swart and Dullemond, the branching ratio  $\Sigma^0/(\Sigma^0+\Lambda)$  obtained is 0.24, compared with the observed ratio  $0.037 \pm 0.022$ . The uncertainties in the comparison between the observed and calculated ratios are discussed in detail, especially those concerned with the validity of the impulse approximation, in view of the near-resonant  $\Sigma N$  interaction in the global symmetry model, and the question of the appropriate form of the spin average, in view of the strong electromagnetic spin-orbit forces in the  $\Sigma^-d$  atom. It is concluded that the appropriate spin average is  $\frac{2}{3}[\Sigma^0/(\Sigma^0+\Lambda)]_{S=3/2} + \frac{1}{3}[\Sigma^0/(\Sigma^0+\Lambda)]_{S=1/2}$  within corrections of about 10%. Agreement with the experimental ratio appears unlikely with global symmetry, even when these uncertainties are taken into account.

### I. INTRODUCTION

IN experimental work on the processes

$$\Sigma^- + d \rightarrow \Sigma^0 + n + n, \quad (1.1a)$$

$$\Sigma^- + d \rightarrow \Lambda + n + n, \quad (1.1b)$$

the quantity convenient to measure is the branching ratio

$$r = N(\Sigma^0)/[N(\Sigma^0) + N(\Lambda)], \quad (1.2)$$

where  $N(Y^0)$  is the number of final  $Y^0$  hyperons. The experimental value of  $r$  for capture at rest, i.e., from bound states of a  $\Sigma^-d$  atom, is<sup>1</sup>

$$r_b(\text{exp}) = 0.037 \pm 0.022. \quad (1.3)$$

Day, Snow, and Sucher made a calculation of  $r_b$  by means of the impulse approximation.<sup>2</sup> They assumed capture from initial  $s$ -wave Bohr orbits, and that the relative  $\Sigma\Lambda$  parity is even and wrote the amplitude for the reaction  $\Sigma^- + p \rightarrow Y^0 + n$  as

$$a_0(Y^0) + a_1(Y^0)\sigma_N \cdot \sigma_Y, \quad (1.4)$$

where  $a_0(Y^0)$  and  $a_1(Y^0)$  are constants and  $\sigma_N$  ( $\sigma_Y$ ) operates between initial and final nucleon (hyperon) spinors.

From the amplitude (1.4) one can calculate also  $r(\text{H})$ , the ratio for  $\Sigma^-$  capture in hydrogen. For  $\Sigma^-$  coming to rest in hydrogen, the experimental value is<sup>3</sup>

$$r_b(\text{H}; \text{exp}) = 0.33 \pm 0.05. \quad (1.5)$$

\* A thesis submitted to the Department of Physics, the University of Chicago, in partial fulfillment of the requirements for the Ph.D. degree.

† This work was supported by the U. S. Atomic Energy Commission at the University of Chicago.

‡ National Science Foundation Predoctoral Fellow.

§ Present address: Department of Physics, University of California, Berkeley, California.

<sup>1</sup> O. Dahl, N. Horowitz, D. Miller, and J. Murray, Phys. Rev. Letters **4**, 77 (1960).

<sup>2</sup> T. B. Day, G. A. Snow, and J. Sucher, Phys. Rev. Letters **2**, 468 (1959).

<sup>3</sup> R. H. Ross, Bull. Am. Phys. Soc. **3**, 335 (1958).

The calculated  $r_b$  and  $r_b(\text{H})$  were, therefore, expressed in terms of three adjustable parameters [two for each final hyperon, less one because  $r_b$  and  $r_b(\text{H})$  are ratios]. Still, it proved impossible to reconcile the two measured numbers.

Chen<sup>4</sup> improved the calculation of reference 2 in two respects: He used a more accurate deuteron wave function, and (more important) he included the effects of the  ${}^1S_0$  force between the two final neutrons. Since the energy release in the  $\Sigma^0$  case is so small (0.94 MeV), the two neutrons always emerge with low relative momentum; the strongly attractive forces at these energies enhance  $N(\Sigma^0)$  by a factor of about 5. He could then obtain a fit to the experimental  $r_b(\text{H})$  and  $r_b$ .

The present paper is motivated in part by a new consideration. Recently, there has been considerable interest in calculating hyperon-nucleon scattering from first principles. de Swart and Dullemond<sup>5,6</sup> have related  $YN$  scattering to nucleon-nucleon scattering by means of global symmetry, and de Swart and Iddings<sup>7,8</sup> have calculated the  $YN$  scattering amplitudes as a function of the  $\pi YN$  coupling constants. This work indicates that, in channels containing final  $\Lambda$  particles, tensor forces can contribute as much to the rate  $N(\Lambda)$  as do the terms (1.3). Already from one-pion exchange one obtains a strong tensor force. Accordingly, in Sec. 2 we calculate  $r_b$  from a matrix element for  $\Sigma^- + p \rightarrow Y^0 + n$  having the form

$$\begin{aligned} \langle p_{Yn} | M | p_{\Sigma p} \rangle \\ = \chi_f [A_S^Y P_S + A_T^Y P_T^Y \\ + D^Y (p_{Yn}^2 \sigma_N \cdot \sigma_Y - 3 p_{Yn} \cdot \sigma_N p_{Yn} \cdot \sigma_Y) / 2^{3/2}] \chi_i. \end{aligned} \quad (1.6)$$

Here  $A_S^Y$ ,  $A_T^Y$ , and  $D^Y$  are, in general, functions of

<sup>4</sup> Y. Y. Chen, Nuovo Cimento **19**, 36 (1961).

<sup>5</sup> J. J. de Swart and C. Dullemond, Ann. Phys. (N. Y.) **16**, 263 (1961).

<sup>6</sup> J. J. de Swart and C. Dullemond, Ann. Phys. (N. Y.) (to be published).

<sup>7</sup> J. J. de Swart and C. Iddings, Phys. Rev. **128**, 2810 (1962).

<sup>8</sup> J. J. de Swart and C. Iddings, preceding paper, Phys. Rev. **130**, 319 (1963).

energy.  $P_S$  and  $P_T$  are singlet and triplet spin projection operators:

$$P_S = \frac{1}{4}(1 - \boldsymbol{\sigma}_N \cdot \boldsymbol{\sigma}_Y), \quad (1.7a)$$

$$P_T = \frac{3}{4}(3 + \boldsymbol{\sigma}_N \cdot \boldsymbol{\sigma}_Y). \quad (1.7b)$$

The first two terms of (1.5) are readily seen to be the earlier matrix element (1.4) rewritten so as to be more easily comparable to references 5-8. Since the tensor term is proportional to  $p_{Yn}^2$ , it need not be considered in computing  $N(\Sigma^0)$ , where the momentum available to the final state is small.

We wish to point out that in the earlier work the ratios  $r$  for capture from bound state were calculated from formulas which actually apply only to capture in flight [we denote the latter ratios by  $r_f$  and  $r_f(H)$ ]. In Sec. 2 this situation is corrected. As a result of this change the conclusion reached by Chen,<sup>4</sup> that the data can be fitted only if values of  $a_0(\Lambda)$ ,  $a_1(\Lambda)$  differing considerably from  $a_0(\Sigma^0)$ ,  $a_1(\Sigma^0)$  are employed, is found no longer to hold. In fact, these data could now be fitted if the parameters were similar in magnitude.

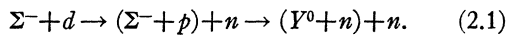
In Sec. 3 the parameters of Eq. (1.6) are obtained from the calculations of de Swart and Dullemond,<sup>6</sup> and  $r_b$  is calculated and compared to experiment.

Section 4 discusses a spin-orbit effect which might alter the theoretical expression for  $r_b$  by introducing transitions between initial bound states of different total spin.

For clarity of presentation, we discuss in the body of the paper only  $\Sigma^-$  capture in deuterium. Results for  $\Sigma^-$  capture in hydrogen have been collected together in an Appendix.

## II. CAPTURE RATE IN DEUTERIUM

The impulse approximation considers reaction (1) to occur in two steps,



The first step, the virtual breakup of the deuteron into its composite particles, is governed by the wave function

$$\langle r | d \rangle = N(e^{-\alpha r} - e^{-\beta r})/r \quad (2.2)$$

in the Hulthén approximation; or in momentum space

$$\langle p | d \rangle = 4\pi N[(\alpha^2 + p^2)^{-1} - (\beta^2 + p^2)^{-1}]. \quad (2.3)$$

The second step, reaction of the  $\Sigma^-$  hyperon, is taken to be determined by the matrix element equation (1.6) for the two-body process  $\Sigma^- + p \rightarrow Y^0 + n$ ; such approximation is justified if that matrix element is not sensitive to the small extrapolation off-energy shell which is made and if no serious "multiple scattering" effects occur, i.e., the intermediate neutron is on the average well removed from the point of interaction between  $p$  and  $\Sigma^-$ .<sup>9</sup>

In momentum space, which is more convenient than configuration space for integration of the tensor term,

the impulse approximation amplitude for reaction (1.1) is written<sup>10</sup>

$$A_{\pm}(k, q) = \int \frac{d^{(6)}p' d^{(6)}p}{(2\pi)^{12}} \langle nnY^0; \mathbf{kq}; \pm | p' \rangle \times \langle p' | M | p \rangle \langle p | \Sigma^- d \rangle, \quad (2.4)$$

with

$$\langle p | \Sigma^- d \rangle = (2\pi)^3 \psi_{nS}(0) \delta^{(3)}(\mathbf{p}_\Sigma) \langle p_{nn} | d \rangle, \quad (2.5)$$

$$\langle p' | M | p \rangle = (2\pi)^3 \delta^{(3)}(\mathbf{p}_s' - \mathbf{p}_s) \langle p_{nY'} | M | p_{\Sigma p} \rangle. \quad (2.6)$$

$p_s$  is the momentum of the "spectator" neutron, non-interacting in the second step of reaction (1.1)

$$\langle p' | nnY^0; \mathbf{kq}; - \rangle = (2\pi)^6 [\delta^{(3)}(\mathbf{k} - \mathbf{p}_{nn}') \delta^{(3)}(\mathbf{q} - \mathbf{p}_{Y'}) - (\mathbf{k} \rightarrow -\mathbf{k})], \quad (2.7)$$

$$\langle p | nnY^0; \mathbf{kq}; + \rangle = (2\pi)^3 \left\{ (2\pi)^3 \delta^{(3)}(\mathbf{k} - \mathbf{p}_{nn}') + (e^{-i\delta} \sin\delta) \times \frac{4\pi}{k} \left[ \frac{1}{p_{nn}^2 - (k - i\epsilon)^2} - \frac{1}{p_{nn}^2 + \lambda^2} \right] \right\} \times \delta^{(3)}(\mathbf{q} - \mathbf{p}_Y) + (\mathbf{k} \rightarrow -\mathbf{k}). \quad (2.8)$$

The bracket  $(\mathbf{k} \rightarrow -\mathbf{k})$  signifies the term obtained from the preceding one by changing the sign of  $\mathbf{k}$ . The wave function for the two final neutrons is either antisymmetrized [Eq. (2.7)] if for triplet  $nn$  spin states or symmetrized [Eq. (2.8)] if for singlet  $nn$  spin states. The latter wave function is an ingoing wave solution to the  ${}^1S_0$   $nn$  scattering problem. In configuration space, this wave function has the form

$$\langle r | nn; \mathbf{k}; + \rangle = [e^{i\mathbf{k} \cdot \mathbf{r}} + e^{-i\mathbf{k} \cdot \mathbf{r}} + 2e^{-i\delta} \sin\delta (e^{-i\mathbf{k}r} - e^{-\lambda r}) (kr)^{-1}], \quad (2.9)$$

where

$$e^{-i\delta} \sin\delta = k[-1/a + r_0 k^2/2 + ik]^{-1}. \quad (2.10)$$

The term containing  $\lambda$  in Eq. (2.9) takes into account the finite range of the nuclear force. When Eq. (2.9) is inserted into the effective range integral, one finds

$$r_0 = 3/\lambda - 4/a\lambda^2. \quad (2.11)$$

Here  $a$  and  $r_0$  are the  ${}^1S_0$  threshold scattering length and effective range deduced from  ${}^1S_0$   $np$  and  $pp$  scattering:  $a = -23.7$  F,  $r_0 = 2.65$  F. From these we deduce the value  $\lambda = 1.18$  F<sup>-1</sup>.<sup>11</sup>

In this paper we consider  $\Sigma^-$  hyperons initially in  $S$ -wave Bohr orbits, or else in  $S$  wave in the continuum at vanishingly small momentum relative to the deuteron center of mass. In both cases, it is suitable to approximate the functions  $A_S^Y$ ,  $A_T^Y$ , and  $D^Y$  in Eq. (1.5) by their values at zero  $\Sigma^- p$  relative momentum. Of course, as the momentum distribution equation (2.3) indicates,

<sup>10</sup> When the same momentum appears both initially and finally, a prime will be used to distinguish the final value; when both a measurable value and a variable of integration in a sum over intermediate states appear in the same expression, a  $p$  will be used for the latter. These distinctions will be dropped when there is no danger of confusion.

<sup>11</sup> 1 F<sup>-1</sup> = 197 MeV/c = 10<sup>13</sup> cm<sup>-1</sup>.

<sup>9</sup> G. F. Chew and G. C. Wick, Phys. Rev. **85**, 636 (1952); G. F. Chew and M. L. Goldberger, *ibid.* **87**, 778 (1952).

the proton is not completely at rest. Usually the variation in  $M$  over this range of momentum is small, so that  $M$  is assumed constant in the present section. Situations in which an energy dependence of  $M$  could be important are discussed in the conclusion to this paper.

The capture rate is given in terms of  $A_{\pm}(k, q)$  by

$$\Gamma_{i\pm} = 2\pi \int \sum_f |\chi_f A_{\pm} \chi_i|^{2\frac{1}{2}} (2\pi)^{-6} d\mathbf{k} d\mathbf{q} \delta(E_i - E_f). \quad (2.12)$$

For the moment there is no need to consider the  $A_S, A_T$  terms in (1.5). Their contribution to  $\Gamma_{i\pm}$  has been computed by Chen.<sup>4</sup> Further, there are no interference terms between them and the tensor term; these cancel when the angular integrations in (2.12) are carried out.

The notation  $A_{ij\pm}$  is introduced for the second-rank tensor which results when, in Eqs. (1.5) and (2.4), the  $A_S^Y, A_T^Y$  terms are ignored and a factor  $(\sigma_N)_i (\sigma_Y)_j$  is removed from the tensor term which remains. Then

$$\int d\mathbf{k} d\mathbf{q} A_{ij\pm}^* A_{k\ell\pm} \delta = (4\pi)^4 N^2 |\psi_{nS}|^2 m_{\Lambda(nn)} (2m_{nn} Q_{\Lambda})^2 |D|^2 M_{ijkl} \times \begin{cases} (T_1 + T_2 + T_3), & \text{subscript } + \\ (T_1 - T_2), & \text{subscript } - \end{cases} \quad (2.13)$$

where

$$M_{ijkl} = (4\pi)^{-1} \int d\Omega (\delta_{ij} - 3\hat{p}_i \cdot \hat{p}_j) (\delta_{kl} - 3\hat{p}_k \cdot \hat{p}_l) / 8 = \frac{3}{40} [\delta_{ik} \delta_{jl} + \delta_{il} \delta_{jk} - \frac{2}{3} \delta_{ij} \delta_{kl}], \quad (2.14)$$

$$m_{a(bc)} = m_a (m_b + m_c) (m_a + m_b + m_c)^{-1}, \quad (2.15)$$

$$2m_{nn} Q_{\Lambda} = m_n [m_p - m_n + m_{\Sigma^-} - m_{\Lambda} - B], \quad (2.16)$$

$$T_1 = 2 \int_0^1 k^2 q dk \{ [(c_1 k)^4 + (c_2 q)^4] C_0 + (c_1 c_2 k q)^2 (8C_2 + 10C_0) \times \frac{1}{3} - 4c_1 c_2 k q [(c_1 k)^2 + (c_2 q)^2] C_1 \}, \quad (2.17)$$

$$T_2 = 2 \int_0^1 k^2 q dk \{ [(c_1 k)^4 + (c_2 q)^4] C_0' + (c_1 c_2 k q)^2 [4C_2' - 10C_0'] \times \frac{1}{3} \}, \quad (2.18)$$

$$T_3 = 2 \int_0^1 k^2 q dk \{ \frac{1}{2} [(\text{Im}H)^2 - (\text{Re}H)^2] \sin^2 \delta + (\text{Im}H)(\text{Re}H) \cos \delta \sin \delta \}, \quad (2.19)$$

$$C_0 = [D(\alpha)^2 - (kq)^2]^{-1} - (\beta^2 - \alpha^2)^{-1} (kq)^{-1} L(\alpha) + (\alpha \leftrightarrow \beta), \quad (2.20)$$

$$C_1 = -\frac{1}{2} \frac{D(\alpha) + D(\beta)}{(kq)^2 (\beta^2 - \alpha^2)} L(\alpha) - \frac{D(\alpha)}{(kq) [D(\alpha)^2 - (kq)^2]} + (\alpha \leftrightarrow \beta), \quad (2.21)$$

$$C_2 = -\frac{1}{2} \frac{(kq)^2 - 3D(\alpha)D(\beta)}{(kq)^3 (\beta^2 - \alpha^2)} L(\alpha) + \frac{P_2[D(\alpha)/kq]}{D(\alpha)^2 - (kq)^2} + (\alpha \leftrightarrow \beta), \quad (2.22)$$

$$C_0' = \frac{1}{2} \frac{\beta^2 - \alpha^2}{kq D(\alpha) [D(\alpha) + D(\beta)]} L(\alpha) + (\alpha \leftrightarrow \beta), \quad (2.23)$$

$$C_2' = -\frac{1}{2} \frac{(\beta^2 - \alpha^2) P_2[D(\alpha)/kq]}{kq D(\alpha) [D(\alpha) + D(\beta)]} L(\alpha) + (\alpha \leftrightarrow \beta), \quad (2.24)$$

$$D(\alpha) = \alpha^2 + k^2 + \frac{1}{4} q^2, \quad (2.25)$$

$$L(\alpha) = \ln \left[ \frac{D(\alpha) + kq}{D(\alpha) - kq} \right], \quad (2.26)$$

$$c_1 = m_{\Lambda} / (m_{\Lambda} + m_n); \quad c_2 = \frac{1}{2} (m_{\Lambda} + 2m_n) / (m_{\Lambda} + m_n). \quad (2.27)$$

$P_2(x)$  is the ordinary Legendre polynomial.

$$\text{Re}H = c_1^2 \frac{k}{q} \left\{ P_2[D(\alpha)/kq] L(\alpha) - \frac{D(\alpha)}{kq} \right\} + 2c_1 c_2 \left[ \frac{D(\alpha)}{kq} L(\alpha) - 2 \right] + c_2^2 \frac{q}{k} L(\alpha) - (\alpha \leftrightarrow \beta), \quad (2.28)$$

$$\text{Im}H = \left\{ 2c_1^2 \frac{k}{q} P_2[D(\alpha)/kq] + 4c_1c_2 \frac{D(\alpha)}{kq} + \frac{2c_2^2q}{k} \right\} \left[ \tan^{-1}\left(\frac{\frac{1}{2}q+k}{\alpha}\right) + \tan^{-1}\left(\frac{\frac{1}{2}q-k}{\alpha}\right) \right] - 4 \tan^{-1}\left(\frac{\frac{1}{2}q}{\alpha+\lambda}\right) \frac{q}{k} \\ \times \left\{ \frac{3}{2} \left(\frac{c_1\lambda}{q}\right)^2 \left[ \left(\frac{\alpha^2 + \frac{1}{4}q^2 - \lambda^2}{\lambda q}\right)^2 + \frac{1}{3} \right] + 2c_1c_2 \left(\frac{\alpha^2 + \frac{1}{4}q^2 - \lambda^2}{q^2}\right) + c_2^2 \right\} - \frac{c_1}{k} \left[ 3c_1\alpha \frac{(k^2 + \lambda^2)}{q^2} + 4c_2\lambda \right] - (\alpha \leftrightarrow \beta). \quad (2.29)$$

The factor  $(2m_{nn}Q_\Lambda)^2$  appears in Eq. (1.13) when quantities in the integrands of the  $T_1, T_2, T_3$  are expressed in units of  $k_{\max} = (2m_{nn}Q_\Lambda)^{1/2}$  [hence, the limits of integration 0 to 1 in Eqs. (2.17)–(2.19)] and originates in the angular momentum barrier against transitions to final  $D$ -wave states. Using it we find that these final states contribute insignificantly to  $\Sigma^0$  production; i.e., the  $\Sigma^0$  tensor contribution is down by four orders of magnitude from the  $\Lambda$  and the nontensor  $\Sigma^0$  contributions:

$$(Q_\Sigma/Q_\Lambda)^2 = (0.941/77.1)^2 = 1.49 \times 10^{-4}. \quad (2.30)$$

The integrals  $T_i$  were integrated on an IBM 1620 digital computer; the results are presented in Table I.

A remark is in order on the value of the deuteron parameter  $\beta$  which we use. It is the one found in the older literature,  $\beta = 6.2\alpha = 1.44 \text{ F}^{-1}$ , a value which fits the  ${}^3S_1$   $np$  effective range.<sup>12</sup> At an earlier stage of the present calculation some work was done with a value  $\beta = 1.20$ .<sup>13</sup> Apparently this latter value was intended by

TABLE I. Tensor force integrals  $T_i$  for final  $\Lambda$  states. Tensor force terms for final  $\Sigma^0$  states are too small to affect the  $\Sigma^0$  rate measurably.

$T_1 + T_2$	4.067
$T_1 - T_2$	3.79
$T_1 + T_2 + T_3$	5.274

its authors to furnish a better fit to the data on elastic  $e-d$  scattering. These data require a repulsion between nucleons at small distances,<sup>14</sup> and small distances ( $r < 0.2 \text{ F}$ ) are indeed suppressed by decreasing  $\beta$ . Simultaneously, however, the asymptotic region  $r > 1/\beta \text{ F}$  is unduly enhanced. The effective range calculated with this wave function is in error by +16%. A more sophisticated parameterization would leave the asymptotic region unchanged while enhancing only the intermediate region,  $0.2 \text{ F} < r < 1/\beta \text{ F}$ . Of course, behavior of  $\langle r | d \rangle$  for  $r < 0.2 \text{ F}$  is hardly important to the present problem; in fact, it is difficult to imagine a problem of any sort to which a two-parameter wave function would apply when it is inaccurate in the asymptotic region. The inclusion of this parameterization into the deuteron literature is to be lamented.

The expressions for  $r_f$  and  $r_b$  can now be derived. We

<sup>12</sup> L. Hulthén and M. Sugawara, in *Handbuch der Physik*, edited by S. Flügge (Springer-Verlag, Berlin, 1957), Vol. 39.

<sup>13</sup> M. J. Moravcsik, Nucl. Phys. I, 113 (1958).

<sup>14</sup> J. I. Friedman, H. W. Kendall, and P. A. M. Gram, III, Phys. Rev. 120, 992 (1960).

discuss this step more fully than is usual because in references 2 and 4,  $r_f$  was used where  $r_b$  applies.

In reactions in flight (capture from bound states), each  $\Sigma^-$  interacts with a very large number of deuterons (only one deuteron). In consequence, the initial state is a statistical distribution over spins (is a state of one definite total spin). Therefore, in flight,

$$-dN(\Sigma^-)/dt = (\sum_i \Gamma_i g_i) N(\Sigma^-), \\ +dN(Y^0)/dt = (\sum_i \Gamma_i Y g_i) N(\Sigma^-), \quad (2.31)$$

and for a bound state

$$-dN_i(\Sigma^-)/dt = \Gamma_i N_i(\Sigma^-), \\ +dN_i(Y^0)/dt = \Gamma_i N_i(\Sigma^-). \quad (2.32)$$

These equations can be integrated readily to give

$$r = [\sum_i N_i(\Sigma^0)] / \{ \sum_i [N_i(\Sigma^0) + N_i(\Lambda)] \}, \\ r_f = (\sum_i g_i \Gamma_i^2) / (\sum_i g_i \Gamma_i), \quad (2.33)$$

$$r_b = \sum_i (g_i \Gamma_i^2 / \Gamma_i). \quad (2.34)$$

The  $g_i$  appear in the equation for  $r_b$  because of the boundary condition  $N_i(\Sigma^-)/N(\Sigma^-)_{t=0} = g_i$ .

It is easy to see that Eqs. (2.33) and (2.34) can differ widely in their predictions for special cases. For example, if there are two spin states and  $\Gamma_1^2 \approx \Gamma_1 \gg \Gamma_2 \gg \Gamma_2^2$ , then Eq. (2.33) predicts that almost all final hyperons will be  $\Sigma^0$ , while Eq. (2.34) predicts that at most the fraction  $g_1$  will be  $\Sigma^0$ .

We compute  $r_f$  and  $r_b$  when the initial states  $i$  are  $S$  wave, total  $\Sigma-d$  spin  $S = 1/2$  (subscript  $D$  for doublet) or  $S = 3/2$  (subscript  $Q$  for quartet). For this choice of initial states  $i$ , Eqs. (2.33) and (2.34) become

$$r_f = (\frac{1}{3}\Gamma_D^2 + \frac{2}{3}\Gamma_Q^2) / (\frac{1}{3}\Gamma_D + \frac{2}{3}\Gamma_Q), \quad (2.35)$$

$$r_b = \frac{1}{3}(\Gamma_D^2/\Gamma_D) + \frac{2}{3}(\Gamma_Q^2/\Gamma_Q). \quad (2.36)$$

The tensor terms involve the spin sums

$$a_{XY} = \sum_{ijk} (2S+1)^{-1} \text{Trace}[\sigma_i^X \sigma_j^Y P_X(\Sigma^-d) \\ \times P_i(np) \sigma_k^N \sigma_l^Y P_Y(nn) M_{ijkl}]. \quad (2.37)$$

TABLE II. Spin sums for the tensor terms.  $a_{XY}$  is defined by Eq. (2.37). The subscripts  $X$  and  $Y$  refer to the multiplicities  $(2S+1)$  associated with the total spin of the  $\Sigma-d$  system and the total spin of the final neutrons, respectively;  $Q, T, D$ , and  $S$  stand for the multiplicities quartet, triplet, doublet, and singlet.

$XY$	$QT$	$QS$	$DT$	$DS$
$a_{XY}$	5/8	3/8	1/4	0

The  $P_\alpha(ab)$  are projection operators for those states of the system  $ab$  with total spin  $\alpha$ . The  $a_{XY}$  are given in Table II.

Collecting together the tensor results and including nontensor contributions, we get

$$\begin{aligned} \Gamma_{Q^Y} &= \Gamma_{Q_-^Y} + \Gamma_{Q_+^Y} \\ &= (4/\pi)N^2 |\psi_{nS}(0)|^2 m_{Y(nn)} [(I_1 - I_2) |A_{T^Y}|^2 \\ &\quad + (2m_{nn}Q_Y)^2 |D^Y|^2 \\ &\quad \times [\frac{5}{8}(T_1 - T_2) + \frac{3}{8}(T_1 + T_2 + T_3)], \end{aligned} \quad (2.38)$$

$$\begin{aligned} \Gamma_{D^Y} &= \Gamma_{D_-^Y} + \Gamma_{D_+^Y} \\ &= (4/\pi)N^2 |\psi_{nS}(0)|^2 m_{Y(nn)} [\frac{1}{16}(I_1 - I_2) |A_{T^Y} + 3A_{S^Y}|^2 \\ &\quad + \frac{3}{16}(I_1 + I_2 + I_3) |A_{T^Y} - A_{S^Y}|^2 \\ &\quad + (2m_{nn}Q_Y)^2 |D_Y|^2 \frac{1}{4}(T_1 - T_2)]. \end{aligned} \quad (2.39)$$

The integrals  $I_i$  can be obtained from the integrals  $T_i$ : set  $c_1=0$ ,  $c_2=1$ , and remove a factor  $q^4$  from the integrands of Eqs. (2.17)–(2.19). Their values are given in Table III. The numerical results of reference 4 differ a little from those of the table because of an algebraic error in computing the  $nn$  force terms. In Eq. (A.1) of reference 4, the  $nn$  force terms, i.e., all those involving  $r_0$  and  $a$ , should be multiplied by an over-all factor 2; further, all arctangents involving the parameter  $\lambda$  ( $\beta$  in the notation of reference 4) should be multiplied by an additional factor 2. With these corrections, the expression (A.1), when expanded for small values of  $\lambda$  and  $k$ , has the behavior which would be predicted for it upon examining a similar expansion of the original  $nn$  wave function.

### III. $YN$ REACTION PARAMETERS

In this section we compute  $r_b$  and  $r_f$ , using  $\Sigma^-p$  scattering parameters calculated by de Swart and Dullemond<sup>5,6</sup> under the hypothesis of global symmetry. To take into account a major effect of the symmetry-violating interactions, de Swart and Dullemond obtain the  $YN$  scattering matrix from a Schrödinger equation in which the kinetic energy terms are written with the observed  $\Lambda\Sigma$  mass difference; while the potential energy terms are those linear combinations of the  $NN$  potentials prescribed by global symmetry. Their calculations are carried out for three choices of  $NN$  potentials. The first two agree remarkably in their predictions. The third, an “antiglobal symmetry” potential seems to be excluded by data on low-energy  $^3S_1 \Lambda N$  scattering.<sup>5</sup> In the examples of this section we use the results obtained from one of the first two, an  $NN$  potential due to Hamada.

TABLE III. Nontensor integrals  $I_i$ .

	$\Lambda$	$\Sigma^0$
$I_1 + I_2$	4.74	0.100
$I_1 - I_2$	3.33	$1.19 \times 10^{-3}$
$I_1 + I_2 + I_3$	4.90	0.557

These authors do not take into account in the wave equation the mass splittings between the  $\Sigma$  hyperons. They can, then, employ isotopic spin conservation to reduce considerably the number of independent parameters in their problem; however, near threshold (“threshold” in this section always refers to that for  $\Sigma^-p \rightarrow Y^0n$ ) the reactive and kinematical effects of the mass differences are important.

To correct for these effects, these authors use, in their expression for the scattering matrix  $T$  near threshold, the scattering length and effective range matrices calculated for the case of zero mass difference, but momenta and energies calculated from the kinematics appropriate to the actual case, namely,

$$p_{\Sigma p} = 0, \quad (3.1)$$

$$p_{Yn'} = (2m_{Yn}Q_Y)^{1/2}. \quad (3.2)$$

They have applied this procedure to deduce  $\Sigma^-$  reactions in hydrogen.<sup>6,15</sup> We apply the same procedure to the  $\Sigma^-$  reactions in deuterium, except that we change the energy release  $Q_Y$  from 3.1 and 79.3 MeV to that appropriate for deuterium, 0.94 and 77.1 MeV, to take into account the deuteron binding energy of 2.2 MeV.

We neglect the effective range corrections to the scattering length. In reference 6 the  $T$  matrix is calculated both with and without inclusion of finite-range effects. The two calculations are referred to as Case I and Case II, respectively. If any element of the scattering length matrix is large, that element is modified considerably by these effective range corrections, but the scattering matrix  $T$  is modified hardly at all, and  $r_b$  and  $r_f$  by at most a few percent. We do not quote the results for Case II in deuterium, but for a detailed example, see the discussion by de Swart and Dullemond for  $\Sigma^-$  reactions in hydrogen.<sup>6</sup>

The expression for the scattering matrix is

$$T = -A(E)[1 + ip^{2l+1}A(E)]^{-1}. \quad (3.3)$$

The relation between  $T$  and  $M$ , Eq. (1.6), is

$$\begin{aligned} \langle N'Y' | T | NY \rangle &= i(E_N E_Y E_{N'} E_{Y'})^{1/2} (E_{\text{tot}} \pi)^{-1} \langle N'Y' | M | NY \rangle \\ &\approx i(m_{NY} m_{N'Y'})^{1/2} \pi^{-1} \langle N'Y' | M | NY \rangle. \end{aligned} \quad (3.4)$$

The last approximation holds in the nonrelativistic limit.

$A(E)$  is obtained from the effective-range expansion of the  $K$  matrix,

$$\begin{aligned} p^{l+1/2} K^{-1} p^{l+1/2} &= -A^{-1} + m^{1/2} R m^{1/2} (E - E_0) \\ &= -[A(E)]^{-1}. \end{aligned} \quad (3.5)$$

In accordance with our approximation, we set  $A(E) = A$  in Eq. (3.3), with  $A$  obtained from the expansion of  $K^{-1}$

<sup>15</sup> Such an approach, together with the assumption of zero-range forces, has been used in  $\bar{K}N$  scattering to obtain the effect of the  $\bar{K}^0 K^-$  mass difference: R. H. Dalitz and S. F. Tuan, Ann. Phys. (N. Y.) 8, 100 (1959).

for the case  $Q_\Sigma=0$ . The results of de Swart and Dullemond are given for channels of definite isospin, so that a unitary transformation to basis states of definite charge must first be applied to  $T$ ,  $K$ , and  $A(E)$  before the momenta can be changed.

In evaluating  $p_{\Sigma p}$  and  $p_{Yn}$  as in Eqs. (3.1) and (3.2), we have picked only one set of values of the many which these momenta can assume in deuterium. The spectator neutron can carry off a varying amount of momentum. The general formulas for  $p_{\Sigma p}$  and  $p_{Yn'}$ , therefore, depend on  $p_s'$ ,

$$p_{\Sigma p} = -p_s' m_\Sigma / (m_\Sigma + m_p) \quad (3.6)$$

initially; and for the final momentum either

$$p_{Yn'} = [2m_{Yn}(Q_Y - p_s'^2/2m_{n(Yn)})]^{1/2} \quad \text{(final plane waves),} \quad (3.7)$$

or

$$p_{Yn'} = q_{Y'} + p_s' m_Y / (m_Y + m_n) \quad \text{(final } nm \text{ spherical wave).} \quad (3.8)$$

In Eq. (3.7) we have anticipated a constraint which will be imposed on the final momenta by conservation of energy when the amplitude is inserted into the 3-particle phase-space integral. In Eqs. (3.8) and (3.9), we again invoke the convention of Sec. I that momenta written with a  $p$  ( $q$ ) are virtual (observable).

In the case of the final  $nm$ , spherical wave  $p_s'$ , hence  $p_{Yn'}$ , can assume all values since it is related to  $p_{nn'}$ , the variable of integration which occurs in the Fourier transform of the spherical wave, Eq. (2.8):

$$p_{nn'} = -\frac{1}{2}q_{Y'} - p_s'. \quad (3.9)$$

The choice  $p_{Yn'} = (2m_{Yn}Q_Y)^{1/2}$  is obtained from the general formulas (3.6)–(3.8) by selecting final plane waves and setting  $p_s' = 0$ . This value was chosen because the deuteron momentum distribution favors small values of  $p_s'$ .

Table IV gives the values of  $T$  calculated from Eqs. (3.1)–(3.3) and the  $A$  matrix given by de Swart and Dullemond.<sup>6</sup> One can then convert from  $T$  to  $M$  using

TABLE IV.  $T$  matrix at threshold and  $\Sigma^0$  branching ratios  $r_b$  and  $r_f$  calculated from the  $A$  matrix of de Swart and Dullemond (reference 6). The initial states are either ( $\Sigma^-$ ;  $^3S_1$ ) or ( $\Sigma^-$ ;  $^1S_0$ ) for final  $J=1$  or 0, respectively. The last column gives a shorthand notation for the  $T$ -matrix element in column 1.

Final state	$\langle T \rangle$ (F)	Notation
$\Sigma^0$ ; $^3S_1$	$-1.18i + 0.197$	$\Sigma_T$
$\Sigma^0$ ; $^1S_0$	$3.47i - 1.47$	$\Sigma_S$
$\Lambda$ ; $^3S_1$	$0.534i + 0.328$	$\Lambda_T$
$\Lambda$ ; $^1S_0$	$-0.0722i - 0.244$	$\Lambda_S$
$\Lambda$ ; $^3D_1$	$0.363i + 0.133$	$\Lambda_{TD}$
$r_b$	0.24	
$r_f$	0.25	

Eq. (3.4), and then insert  $M$  into formulas (2.38) and (2.39) to find  $r_b$  and  $r_f$ , also given in Table IV.

No experimental information is available on  $r_f$ . It is seen that the calculated  $r_b$  is larger by roughly a factor 4 than the upper limit on the experimental value  $0.037 \pm 0.022$ .

#### IV. SPIN-STATE MIXING

Because the spin-orbit electromagnetic interaction in the  $\Sigma^-d$  atom is not symmetric in the spins of  $\Sigma^-$  and  $d$ , the total spin

$$|\mathbf{S}| = |\mathbf{s}_+ + \mathbf{s}_-| \\ = 1/2 \text{ or } 3/2, \quad (4.1)$$

in the initial state is not a good quantum number; that is, the initial atomic eigenfunctions are mixtures of quartet ( $S=3/2$ ) and doublet ( $S=1/2$ ) spin eigenfunctions. (Though not those with  $l=0$ , since there is no spin-orbit interaction for  $l=0$ .) In this situation, one can conceive of two mechanisms whereby the expression (1.32) for  $r_b$  would be distorted from its simple form. We take them in turn.

##### A. Mixing During Collisions

At the moment of nuclear capture, it is likely that the atom will be in a strongly polarized state.<sup>16,17</sup> While the  $\Sigma^-d$  atom is polarized, transitions  $l \rightarrow l' \neq l$  are allowed. Therefore, via intermediate states  $l' \neq 0$  a hyperon bound in a  $^4S$  state can change to a  $^2S$  state, or vice versa, e.g.,

$$^4S_{3/2} \rightarrow ^4P_{3/2} \rightarrow ^2P_{3/2} \rightarrow ^2S_{1/2}. \quad (4.2)$$

The spectroscopic notation is  $^{2S+1}L_J$ , i.e.,  $^4S_{3/2}$  is total spin  $S=3/2$ , orbital angular momentum  $l=0$ , total angular momentum  $J=3/2$ . Therefore, the rate of change of the number of doublet spin states depends on the number of quartet states. Equation (2.32), and in consequence the expression (2.34) for  $r_b$  derived from it, is not true exactly if  $i$  indexes total spin.

The error suffered in using states of definite spin will be small if

$$\left| \sum_{\alpha''} \frac{\langle D\alpha | V | Q\alpha'' \rangle \langle Q\alpha'' | V | Q\alpha \rangle}{(E_{D\alpha}^{(0)} - E_{Q\alpha''}^{(0)}) (E_{D\alpha}^{(0)} - E_{Q\alpha}^{(0)})} \right| \ll 1. \quad (4.3)$$

The  $\alpha$  are the quantum numbers other than spin, and superscript (0) denotes quantities computed in the absence of  $V$ .

$$E_{S\alpha}^{(0)} = \omega_{S\alpha} - \frac{1}{2}i\Gamma_{S\alpha}. \quad (4.4)$$

Following Breit,<sup>18</sup> one can write the spin dependence of the  $\Sigma^-d$  electromagnetic interaction as

<sup>16</sup> T. B. Day, G. A. Snow and J. Sucher, Phys. Rev. Letters 3, 61 (1959).

<sup>17</sup> M. Leon and H. A. Bethe, Phys. Rev. 127, 636 (1962).

<sup>18</sup> The Breit equation is discussed in Sec. 42 of H. A. Bethe and E. E. Salpeter, *Quantum Mechanics of 1- and 2-Electron Atoms* (Springer-Verlag, Berlin, 1957).

$$V = V_S + V_{\Delta S}, \quad (4.5)$$

$$V_S = g_+ g_- \mu_N^2 \left[ -\frac{8\pi}{3} \mathbf{s}_+ \cdot \mathbf{s}_- \delta^{(3)}(\mathbf{r}) + (\mathbf{s}_+ \cdot \mathbf{s}_- - 3 \mathbf{s}_+ \cdot \hat{r} \mathbf{s}_- \cdot \hat{r}) \right] \\ \times \frac{1}{r^3} + \frac{1}{2} (g_+' - g_-') \mu_N^2 \frac{1}{r^3} \mathbf{L} \cdot (\mathbf{s}_+ + \mathbf{s}_-), \quad (4.6)$$

$$V_{\Delta S} = -\frac{1}{2} (g_+' + g_-') \mu_N^2 \frac{1}{r^3} \mathbf{L} \cdot (\mathbf{s}_+ - \mathbf{s}_-). \quad (4.7)$$

In Eq. (4.3) terms of first order in  $\langle V \rangle$  have vanished. Because of rotational symmetry about the  $z$  axis, taken along the line from neighbor nucleus to  $\Sigma^-d$  center of mass,  $l_z$  is a conserved quantum number. Only states with  $l_z=0$  will be able to decay, and  $\langle l_z=0 | V_{\Delta S} | l_z=0 \rangle = 0$ .

Matrix elements of  $V_S$  preserve total spin  $S$ ; so also do some elements of  $V_{\Delta S}$ , if  $s_+^2 \neq s_-^2$ . In what follows, we shall ignore spin-preserving elements if they are diagonal in  $S$  and  $\alpha$ ; such elements can only help by further removing the degeneracy between quartet and doublet states.

The  $g$  factors are defined in terms of the proton Bohr magneton  $\mu_N$ ,

$$\mu_N = e\hbar/2m_p c, \quad (4.8)$$

$$\mathbf{u} = g \mathbf{s} \mu_N, \quad (4.9)$$

$g_{\pm} = \pm 2$  for a Dirac particle,  $+5.4$  for a proton,  $-3.7$  for a neutron,  $+0.957$  for deuterium. The  $g_{\pm}'$  include factors of inverse mass coming from the orbital motion as well as a factor  $m_p$  because the unit of magnetic moment was chosen to be the proton magneton.

$$g_{\pm}' = m_p [1/m_{\pm} + 2/m_{\mp}] g_{\pm}. \quad (4.10)$$

Equations (4.6)–(4.10) would look more familiar if taken to various limits. Two of these are  $m_+ \gg m_-$  and  $g_-/m_p \rightarrow g_-/m_e$  (hydrogen); and  $m_+ = m_-$ ,  $g_+ = -g_-$ ,  $g_{\pm}/m_p \rightarrow g_{\pm}/m_+$  (particle-antiparticle, e.g., positronium).

We estimate  $\langle V \rangle$  and  $\Gamma$  in turn. The order of magnitude of  $\langle V \rangle$  is determined mainly by the factor

$$\mu_N^2 \langle l_n | r^{-3} | l_n \rangle = \frac{2\mu_N^2}{(a_{\Sigma d n})^3} \frac{1}{l(l+1)(2l+1)} \quad (4.11)$$

$$= \frac{9 \times 10^{14}}{n^3} \frac{1}{l(l+1)(2l+1)} \text{ sec}^{-1}. \quad (4.12)$$

Note that in baryonic atoms the distinction between fine and hyperfine structure disappears. The angular factors are of order  $l$ , e.g.,

$$\langle L, S = \frac{1}{2}, l_z S_z | \mathbf{L} \cdot (\mathbf{s}_+ - \mathbf{s}_-) | L, S = \frac{3}{2}, l_z \pm 1, S_z \mp 1 \rangle \\ = \pm \frac{1}{3} [(l \mp l_z)(l \pm l_z + 1)(\frac{3}{2} \mp S_z)(\frac{5}{2} \mp S_z)]^{1/2}, \quad (4.13a)$$

$$\langle L, S = \frac{1}{2}, l_z, S_z | \mathbf{L} \cdot (\mathbf{s}_+ + \mathbf{s}_-) | L, S = \frac{3}{2}, l_z, S_z \rangle \\ = \frac{2}{3} l_z [(\frac{3}{2})^2 - S_z^2]^{1/2}. \quad (4.13b)$$

TABLE V. Estimate of the coupling factors occurring in the spin-dependent part of the electromagnetic interaction in  $\Sigma^-d$  and  $\Sigma^-p$ . The  $\Sigma^-$  hyperon is taken to have the same magnetic moment as the neutron.

	$\Sigma^-d$	$\Sigma^-p$
$g_+ g_-$	-3.6	-20.5
$\frac{1}{2}(g_+' - g_-')$	4.4	8.8
$\frac{1}{2}(g_+' + g_-')$	-2.4	5.0

Finally, there are the coupling factors  $\frac{1}{2}(g_+' \pm g_-')$ ,  $g_+ g_-$ . The  $g$  factor for a  $\Sigma^-$  hyperon is not known. If one chooses it equal to that of the neutron, one gets the values given in Table V. Thus, for  $l=1$  in deuterium, the typical spin-mixing matrix element is

$$|\langle 1n | V_{\Delta S} | 1n \rangle| \approx 4 \times 10^{14} / n^3 \text{ sec}^{-1} \quad (4.14)$$

and falling off rapidly with  $l$ .

For the estimate of  $\Gamma$  we can use the  $T$ -matrix parameters calculated by de Swart and Dullemond for  $\Sigma^-p \rightarrow \Lambda n$  scattering. These parameters are not unusual in order of magnitude and are consistent with the scanty data on the total cross section in hydrogen.<sup>19</sup> We ignore the contribution from final states, as Eq. (1.3) indicates it is small. Using formulas (2.38), (2.39), and (3.4), and the results of Tables I and III, we get

$$\Gamma_Q = \frac{7.52 \times 10^{17}}{n^3} [3.33 |\Lambda_T|^2 + 15.0 |\Lambda_{TD}|^2] \text{ sec}^{-1}, \quad (4.15)$$

$$\Gamma_D = \frac{7.52 \times 10^{17}}{n^3} [0.208 |\Lambda_T + 3\Lambda_S|^2 \\ + 0.918 |\Lambda_T - \Lambda_S|^2 + 3.27 |\Lambda_{TD}|^2] \text{ sec}^{-1}. \quad (4.16)$$

For the key to the notation, see Table IV. The results of de Swart and Dullemond give  $|\Lambda|^2$ 's all of order  $0.1 \text{ F}^2$ , so that

$$\Gamma_Q \approx 1 \times 10^{18} / n^3, \quad (4.17) \\ \Gamma_D \approx 3 \times 10^{17} / n^3.$$

The estimates (4.14) and (4.17) must be transformed from the representation diagonal in  $l$  to a representation in which the  $\alpha$  are diagonal. The eigenfunctions  $|\alpha S\rangle$  will be linear combinations of, in general, all  $l$  values  $l \leq n-1$ . In computing  $\langle \alpha S | V_{\Delta S} | \alpha' S' \rangle$  we neglect contributions from  $D$  and higher waves. Then  $\Gamma$  and  $V_{\Delta S}$ , when evaluated in the  $(\alpha, S)$  representation, will be proportional to the fraction of  $S$  and  $P$  waves, respectively, in the eigenfunctions  $|\alpha S\rangle$ . We assume that the fraction of  $S$  wave in each  $|\alpha S\rangle$  is of the same order of magnitude as the fraction of  $P$  wave. Then estimates (4.14) and (4.17) may be used directly in Eq. (4.3). That criterion is seen to be very well satisfied.

If the  $\Sigma^-d$  atom is small compared to the distance to the neighbor nucleus, then the field at the atom is ap-

<sup>19</sup> G. Alexander, J. Anderson, F. Crawford, W. Laskar, and L. Lloyd, Phys. Rev. Letters 7, 348 (1961).

proximately constant. The eigenfunctions in such a field (those of the linear Stark effect) are well known and may be used to check the assumption that the fraction of  $S$  and  $P$  waves are comparable. Every Stark eigenfunction with  $l_z=0$  has exactly the same fraction of  $S$  wave,  $1/n$ ; the fraction of  $P$  wave varies from 0 to  $3/n$ , the average value being  $\approx 1/n$ .

An approximate degeneracy

$$E_{D\alpha}^{(0)} = E_{Q\alpha}^{(0)} + O(\langle V \rangle) \quad (4.18)$$

would reduce Eq. (4.3) to first order in  $\langle V \rangle$ . Even were this fortuity to occur, the correction due to spin mixing would still be small, of order  $10^{14}/10^{17} = 10^{-3}$ .

### B. Mixing between Collisions

In general, a  $\Sigma^-d$  atom passes through the polarizing field of a neighbor atom sufficiently quickly that some hyperons remain uncaptured after several mean collision times. Suppose there were more doublets than quartets remaining at that time because the quartet capture rate happened to be the faster. Between collisions the spin-state mixing goes on (not prevented by any complex energy difference, since  $l > 0$ ) and tends to restore the number of quartet and doublet states to the statistical distribution. The net result would be that the fraction of hyperons captured from quartet states would be greater than the factor of  $2/3 = g_Q$ , used in Eq. (2.34) for  $r_b$ .

The spin  $S$  amplitude will tend to increase at the expense of the spin  $S' \neq S$  amplitude as  $\sin\langle S' | V_{\Delta S} | S \rangle t$ . Therefore, expression (2.34) for  $r_b$  is an excellent approximation if  $\langle S' | V_{\Delta S} | S \rangle \tau$  is small;  $\tau$  is the mean time spent outside a polarizing field, between initial polarizing collision and final capture.

#### 1. Simple Model

The collision problem is too complex for  $\tau$  to be computed exactly, but the following simple model of the collision should give the order of magnitude. We consider a  $\Sigma^-d$  atom which collides with a polarizing source of effective radius  $R_0$ . Recoil is neglected and the path of the  $\Sigma^-d$  atom is taken as a straight line. The radius  $R_0$  is taken to be that at which the polarizing field first be-

TABLE VI. Factors for computing the amount of mixing of opposite-spin amplitudes  $\langle S' | V_{\Delta S} | S \rangle$ , during transits in field-free space.  $n^3\Gamma = 3 \times 10^{17} \text{ sec}^{-1}$ . The factors missing from  $\tau^{-1}$  and  $\langle S' | V_{\Delta S} | S \rangle$  decrease  $\langle S' | V_{\Delta S} | S \rangle \tau$  by  $\approx (5/n)$ .  $\tau_1^{-1}$  and  $\langle S' | V_{\Delta S} | S \rangle$  are in units of  $10^{10} \text{ sec}^{-1}$ .

$n$	$R_0/a_0$	$\eta R_0$	$\tilde{f}(n)$	$\tau_1^{-1} \tilde{f}(n)$ $\propto \tau^{-1}$	$2\mu_N^2 (a_{\Sigma d} n)^{-3}$ $\propto \langle S'   V_{\Delta S}   S \rangle$
5	1	50	1.0	32	630
8	2	14.7	0.99	130	150
13	3	3.82	0.88	250	40
20	4	0.964	0.46	240	12
30	5	0.234	0.14	110	3.4
37	5.5	0.114	0.076	74	1.8

comes strong enough to overcome the energy splitting  $\omega - \frac{1}{2}i\Gamma$  between  $|n, 0\rangle$  and all states  $|n, l > 0\rangle$ . Inside  $R_0$  the eigenfunctions are assumed to be of Stark form. Bethe and Leon,<sup>17</sup> who have solved the Stark field eigenvalue problem for various decay rates  $\Gamma$  and external fields  $F$ , show that the decay rate of a Stark eigenfunction has reached 0.9 of its strong-field limit  $\Gamma/n$  when the following criterion is satisfied:

$$\frac{2}{3} e a_{\Sigma d} F_0 n^2 = 0.66 (\frac{1}{2}\Gamma), \quad (4.19)$$

$$F_0 = F(R_0) = e R_0^{-2} \int_0^{R_0} e^{-2\rho/a_0} \rho^2 d\rho a_0^{-3} \\ = \frac{e}{R_0^2} \left[ 1 + 2 \left( \frac{R_0}{a_0} \right) + 2 \left( \frac{R_0}{a_0} \right)^2 \right] e^{-2R_0/a_0}. \quad (4.20)$$

We use Eqs. (4.19) and (4.20) to determine  $R_0$ .

If the  $\Sigma^-d$  atom moves along a chord of length  $d$  inside the polarizing region, the fraction of hyperons with  $l_z=0$  captured per pass is

$$f(n) = 1 - \exp(\eta d/2), \quad (4.21)$$

$$\eta = 2\Gamma/n V_{\text{th}}, \quad (4.22)$$

$$V_{\text{th}} = \text{thermal velocity} = 8.5 \times 10^4 \text{ cm/sec } (\Sigma^-d), \quad (4.23)$$

or averaged over all impact parameters,

$$\tilde{f}(n) = 1 - 2[1 - \exp(-\eta R_0)(1 + \eta R_0)](\eta R_0)^{-2}. \quad (4.24)$$

For small  $\eta R_0$  ( $\eta R_0 < 0.2$ ), we use the approximation, good to better than 10%,

$$\tilde{f}(n) \rightarrow \frac{2}{3}\eta R_0 \text{ as } \eta R_0 \rightarrow 0. \quad (4.25)$$

Since  $l_z=0$  is only a fraction  $1/(2l+1)$  of the total number of states with angular momentum  $l$ , it should take of order

$$(2l+1)/\tilde{f}(n) \quad (4.26)$$

collisions to depopulate the level  $(l, n)$ . Now the (mean free time)<sup>-1</sup> between two successive collisions,  $\tau_1^{-1}$ , is calculated from a familiar formula to be

$$\tau_1^{-1} = V_{\text{th}} \pi R_0^2 N, \quad (4.27)$$

where  $N = 4.3 \times 10^{22} \text{ cm}^{-3}$ . Then

$$\tau^{-1} = \tau_1^{-1} \tilde{f}(n) / (2l+1) \\ = 3.4 \times 10^{11} (R_0/a_0)^2 \tilde{f}(n) / (2l+1) \text{ sec}^{-1}. \quad (4.28)$$

We compare  $\tau^{-1}$  and  $\langle S' | V_{\Delta S} | S \rangle$  in Table VI.

It is simpler to choose a value of  $R_0$  and then calculate  $n$  rather than vice versa. This treats  $n$  as a continuous variable; the  $n$  value given in Table VI has there been rounded off to the nearest integer.

A number of considerations determined the range of  $n$  values to be emphasized in the table. To begin with,  $n > 38$  should not be important because this corresponds to a  $\Sigma^-d$  radius  $> a_0$  and we expect the  $\Sigma^-$  hyperon to be captured initially into a Bohr orbit approximating the size of a deuterium atom. Small  $n$  values should not be important either. Bethe and Leon<sup>17</sup> have shown that for



$K^-p$  essentially all mesons have been captured by  $n=4$ , the captures occurring with roughly equal probability from every  $n$  value  $4 \leq n \leq 23$  (the latter corresponding to a  $K^-p$  radius of  $a_0$ ). They show that for  $\pi^-p$ , on the other hand, the captures are bunched toward smaller  $n$  because  $\Gamma$  is smaller and Auger de-excitation faster. We expect the trend indicated by  $K^-p$  to persist to  $\Sigma^-d$ , with perhaps  $n \approx 5$  the lower limit.

Since the hyperon awaiting capture changes its  $l$  value at each collision, the average over  $l$  should be used in computing  $\langle S' | V_{\Delta S} | S \rangle \tau$ :

$$\sum_{l=1}^{n-1} \left( \frac{2l+1}{n^2-1} \right) \frac{1}{2l+1} \frac{\frac{2}{3}\sqrt{2}[l(l+3/2)]^{1/2}}{l(l+1)(2l+1)} \approx \frac{2}{n}. \quad (4.29)$$

Therefore,

$$\langle \langle S' | V_{\Delta S} | S \rangle \tau \rangle_{av} \approx [\tau_1 / \bar{f}(n)] [(2\mu_N)^2 (a_{\Sigma d} n)^{-3}] [\frac{1}{2}(g_+' + g_-' ) (2/n)]. \quad (4.30)$$

In Eq. (4.29) we have used

$$\begin{aligned} \langle {}^2L_{L\pm 1/2} | \mathbf{L} \cdot (\mathbf{s}_+ - \mathbf{s}_-) | {}^4L_{L\pm 1/2} \rangle \\ = (2\sqrt{2}/3) [l(l+3/2)]^{1/2}, \quad j=l+1/2, \\ = (2\sqrt{2}/3) [(l+1)(l-1/2)]^{1/2}, \quad j=l-1/2. \end{aligned} \quad (4.31)$$

Thus, to compute  $\langle S' | V_{\Delta S} | S \rangle$  from Table VII, one should take the ratio of the last two columns, then multiply by the factor  $\frac{1}{2}(g_+' + g_-' ) (2/n) \approx (5/n)$ . Then it follows that spin-mixing need be taken into account only for those mesons which survive down to  $n \leq 8$ .

### 2. Effect of Rotating Coordinate System

We designate the polarizing interaction by  $V_E$ :

$$V_E = -e(\mathbf{r}_+ - \mathbf{r}_-) \cdot \mathbf{F}, \quad (4.32)$$

$$\mathbf{F} = \hat{R}F. \quad (4.33)$$

In order to use the symmetry of  $V_E$  about the field direction, we chose  $\mathbf{R}$  as axis of quantization. This is a moving axis, so that a spatial coordinate in the wave function becomes an explicit function of time:  $\theta = \theta(t)$ , where  $\theta$  is the polar angle between  $\mathbf{R}$  and a fixed axis in the plane of collision. Then on taking the time derivative in the wave equation, one gets what is in effect a new interaction term in addition to  $V_E$ ,

$$V_\theta = -i\dot{\theta} \frac{\partial}{\partial \theta} = \dot{\theta}(L_y + S_y), \quad (4.34)$$

where  $y$  is the axis normal to the plane of collision. The term  $\dot{\theta}S_y$  can change neither  $\tau$  nor  $|S|$  and in the ensuing discussion will be dropped from  $V_\theta$ .  $V_\theta$  is not symmetric about the  $z$  axis, and in contrast to  $V_E$  its matrix elements obey the selection rules  $\Delta l_z = \pm 1$ ,  $\Delta l = 0$ . Further,  $V_\theta$  is Coulomb-like in its  $R$  dependence and will eventually predominate over  $V_E$  for large  $R$ :

$$\begin{aligned} \dot{\theta} &\lesssim V_{th}/R \\ &\approx 2 \times 10^{13} (a_0/R) \text{ sec}^{-1}. \end{aligned} \quad (4.35)$$

TABLE VII. Factors for computing the amount of mixing of opposite-spin amplitudes  $\langle S' | V_{\Delta S} | S \rangle$ , during transits in field-free space.  $n^3\Gamma = 1 \times 10^{18} \text{ sec}^{-1}$ . The factors missing from  $\tau^{-1}$  and  $\langle S' | V_{\Delta S} | S \rangle$  decrease  $\langle S' | V_{\Delta S} | S \rangle \tau$  by  $\approx (5/n)$ .  $\tau_1^{-1}$  and  $\langle S' | V_{\Delta S} | S \rangle$  are in units of  $10^{10} \text{ sec}^{-1}$ .

$n$	$R_0/a_0$	$\eta R_0$	$\bar{f}(n)$	$\tau_1^{-1} \bar{f}(n) \propto \tau^{-1}$	$2\mu_n^2 / (a_{\Sigma d} n)^3 \propto \langle S'   V_{\Delta S}   S \rangle$
5	0.5	$1 \times 10^2$	1.0	8.0	840
7	1	64	1.0	32	310
8			1.0	(56) <sup>a</sup>	175
11	2	18.8	1.0	128	72
17	3	4.86	0.92	267	20
25	4	1.23	0.54	280	5.6
38	5	0.30	0.20	162	1.6

<sup>a</sup> By linear interpolation.

As  $R$  increases, it mixes more of the ( $l > 0, l_z \neq 0$ ) states into the state ( $l > 0, l_z = 0$ ), so that the latter is less able to couple to  $S$  wave. As a result,  $V_\theta$  decreases the interaction radius  $R_0$  in the model of subsection *B.1* to a smaller value  $R_0'$  determined by the new criterion  $V_\theta = V_E$ .

To obtain  $R_0'$ , we need a measure of the ability of  $V_\theta$  to couple Stark eigenfunctions of different  $l_z$ . On examining  $V_E$  and  $V_\theta$  written in the  $l, l_z$  representation,

$$\begin{aligned} V_E = \frac{3}{2} e a_{\Sigma d} F n \left\{ \left[ \frac{(l^2 - l_z^2)(n^2 - l^2)}{(2l+1)(2l-1)} \right]^{1/2} a_{l-1}^{l_z} \right. \\ \left. + \left[ \frac{[(l+1)^2 - l_z^2][n^2 - (l+1)^2]}{(2l+3)(2l+1)} \right]^{1/2} a_{l+1}^{l_z} \right\}, \end{aligned} \quad (4.36)$$

$$\begin{aligned} V_\theta = -\frac{i}{2} \dot{\theta} \{ [l(l+1) - l_z(l_z-1)]^{1/2} a_l^{l_z-1} \\ - [l(l+1) - l_z(l_z+1)]^{1/2} a_l^{l_z+1} \}. \end{aligned} \quad (4.37)$$

We note that each term from  $V_E$  and  $V_\theta$  comes out to be approximately  $\frac{3}{2} e a_{\Sigma d} F n^2$  and  $\frac{1}{2} \dot{\theta} n$ , respectively, if the quantities  $(n^2 - l^2)^{1/2}$ , etc., are summed over  $l, l_z$  by a rough procedure, replacing  $l$  and  $l_z$  by continuous variables and integrating. As criterion for determining  $R_0'$ , therefore, we take

$$\frac{3}{2} e a_{\Sigma d} F_0' n^2 = \frac{1}{2} \dot{\theta}_0' n, \quad (4.38)$$

where

$$\dot{\theta}_0' = V_{th}/R_0', \quad (4.39)$$

$$F_0' = F(R_0'). \quad (4.40)$$

TABLE VIII. The interaction radius of a neighbor atom, considered as a polarizing source, changes from  $R_0$  to  $R_0'$  if the region in which  $V_\theta > V_E$  is ignored. The last column gives the maximum increase in  $\langle S' | V_{\Delta S} | S \rangle \tau$  to be expected from this decrease in radius.  $n^3\Gamma = 3 \times 10^{17} \text{ sec}^{-1}$ .

$n$	$R_0/a_0$	$\frac{1}{2} \dot{\theta}_0 n / \frac{3}{2} e a_{\Sigma d} F_0 n^2$	$R_0'/a_0$	$(R_0/R_0')^3$
37	5.5	32	3.6	3.6
30	5	16	3.5	2.9
20	4	4.0	3.25	1.9
13	3	0.98	...	...

TABLE IX. The interaction radius of a neighbor atom, considered as a polarizing source, changes from  $R_0$  to  $R_0'$  if the region in which  $V_\theta > V_E$  is ignored. The last column gives the maximum increase in  $\langle S'|V_{\Delta S}|S\rangle\tau$  to be expected from this decrease in radius.  $n^2\Gamma = 1 \times 10^{18} \text{ sec}^{-1}$ .

$n$	$R_0/a_0$	$\frac{1}{2}\theta_0 n / \frac{3}{2}ea\Sigma_d F_0 n^2$	$R_0'/a_0$	$(R_0/R_0')^3$
38	5	12	3.6	2.6
25	4	3.1	3.35	1.7
17	3	0.78	...	...

Note that  $V_E/V_\theta$  falls off rapidly with  $R$ , so that  $R_0$  and  $R_0'$  should not differ by factors as great as orders of magnitude.

$$V_E/V_\theta \propto e^{-2R/a_0} [1 + 2(R/a_0) + 2(R/a_0)^2] R^{-1}. \quad (4.41)$$

$R_0'$  is given in Tables VIII and IX. In the final column of each table we compute  $(R_0/R_0')^3$ , which is the resultant increase in  $\langle S'|V_{\Delta S}|S\rangle\tau$  [in  $\tau^{-1}$  there is a factor of  $R_0^2$  from the collision cross section, as well as additional  $R_0$  dependence, amounting to another factor of at most  $R_0$ , from the factor of  $f(n)$ ]. For levels  $n \leq 13$ , the criterion  $V_\theta = V_E$  is less restrictive than the previous criterion. For levels  $n > 13$  we see on referring back to Table VI that even with the additional factor  $(R_0/R_0')^3$ ,  $\langle S'|V_{\Delta S}|S\rangle\tau$  is still not of order unity. Therefore, our previous conclusion, that spin mixing will be important only for those which survive down to  $n \leq 8$ , is unaltered. However, in the remainder of this section we will include the factor  $(R_0/R_0')^3$  in our estimates of  $\tau$ .

### 3. Hyperons Surviving to $n=8$

We can neglect quartet-doublet transitions occurring for  $n > 8$ , especially since the hyperon spends even less than a capture lifetime in any of these states, due to the cascading. The time between arrival at  $n \leq 8$  and capture, however, will be sufficient for thorough mixing.

One collision, after  $n \leq 8$ , suffices to capture the  $\Sigma^-$  since  $f(n) \approx 1$  for this range of  $n$  values. During this terminating collision, a fraction  $\delta$  of the initially doublet  $\Sigma^-$  will be captured from quartet states,

$$\delta = \frac{2}{3} [N_D(8)/N_D(38) - N_Q(8)/N_Q(38)] \quad (4.42)$$

$r_b$  will be given, not by Eq. (2.36), but by

$$\frac{2}{3} (1 + \frac{1}{2}\delta) \Gamma_Q^2 / \Gamma_Q + \frac{1}{3} (1 - \delta) \Gamma_D^2 / \Gamma_D. \quad (4.43)$$

In deuterium  $\Gamma_Q^2 \ll \Gamma_D^2$ : initial quartet states are allowed by angular momentum conservation to reach only those final  $mn$  states which have triplet spin, therefore,  $P$  wave or higher; while initial doublet states can reach  $S$ -wave final  $mn$  states. Consequently, the first term in Eq. (4.43) is negligible, and it follows that

$$\Delta r_b / r_b \approx \delta. \quad (4.44)$$

The depletion  $N(8)/N(38)$  is computable if  $\tau^{-1}$  and the rate of cascading are known. The two cascade mechanisms which predominate for large  $n$  are (a)

inelastic collision with ejection of an electron, important for  $5 \lesssim n \lesssim 28$  (Auger effect); and (b) inelastic collision with dissociation of the neighbor molecule, important for  $28 \lesssim n \lesssim 38$ .

Bethe and Leon<sup>17</sup> have calculated in Born approximation Auger rates  $\Gamma_A$  for  $\pi^-p$  and  $K^-p$ . We shall scale their results for the case of the  $\Sigma^-d$  system. Writing only the factors in  $\Gamma_A$  which depend upon the characteristics of the atom being polarized, we have

$$\Gamma_A \propto \sum_{l,l'} |\langle n'l' | r_{\Sigma d} | nl \rangle|^2 [\Delta E_{\Sigma d} + 3.7 \text{ eV}]^{-1/2}. \quad (4.45)$$

The first factor comes from the coupling of the  $\Sigma^-d$  charge distribution, approximated by its dipole moment, to a virtual Coulomb photon. The radical comes from numerical integration over factors containing (electron momentum)<sup>2</sup>  $\propto \Delta E_{\Sigma d}$ : a phase-space factor times a squared matrix element, from the coupling of the virtual photon to the deuterium electron. Since  $\Delta E_{\Sigma d} > 15.2 \text{ eV}$  (here we use the ionization energy of the deuterium molecule rather than 13.6 eV, that of the atom), we can neglect the 3.7 eV in computing the scaling factor. Then

$$\Gamma_A^{\Sigma d} = \left( \frac{n_{\Sigma d}}{n_{Kp}} \right)^{5.5} \left( \frac{m_{Kp}}{m_{\Sigma d}} \right)^{2.5} \Gamma_A^{Kp} \quad \text{for fixed } \Delta n = n' - n, \quad (4.46)$$

where we use

$$\Delta E \approx e^2 \Delta n / a n^3, \quad (4.47)$$

and we conjecture the dipole moment goes as

$$\langle r \rangle \propto n^2 m, \quad (4.48)$$

since the  $n$ th Bohr radius is proportional to  $n^2$ . The  $n$  dependence (4.47)–(4.48) fits well the tables of  $\Gamma_A^{Kp}$  compiled by Bethe and Leon using exact  $\langle n' | r | n \rangle$ ; e.g., for  $\Delta n = 2$ ,  $n \leq 5 \leq 14$ ,  $0.37 \times 10^{10} \text{ sec}^{-1} \leq \Gamma_A \leq 430 \times 10^{10} \text{ sec}^{-1}$  the rule  $\Gamma_A^{Kp} \propto n^{5.5}$  is good to within a factor of 4; for  $\Delta n = 1$ ,  $5 \leq n \leq 11$ ,  $2.5 \times 10^{11} \text{ sec}^{-1} \leq \Gamma_A^{Kp} \leq 290 \times 10^{11} \text{ sec}^{-1}$  it is good to within a factor of 2. To obtain  $\Gamma_A^{\Sigma d}$ , then, we first compute  $\min(\Delta n)$ , the minimum  $n - n'$  which supplies 15.2 eV, for each  $n$ , for  $\Sigma^-d$ . There will be

TABLE X. Auger rates for levels in  $\Sigma^-d$ ; extrapolated by means of formula (4.51) from Auger rates for levels in  $K^-p$  with same  $\min(\Delta n)$  = minimum change in  $n$  value which produces sufficient energy to ionize a neighbor electron. The rates are in units of  $10^{10} \text{ sec}^{-1}$  and are evaluated at the mean of the corresponding  $n$  ranges; the  $\Gamma_A^{Kp}$  are the interpolated values when the mean  $n$  is half-integral.

Min $(\Delta n)$	$K^-p$ $n$ range	$\Sigma^-d$ $n$ range	$\Gamma_A^{Kp}$	$\Gamma_A^{\Sigma d}$
6	21	28–27	15	8.5
5	20	26–24	41	18
4	19–17	23–21	70	27
3	16–15	20–19	125	55
2	14–12	18–15	310	150
1	11–10	14–13	2400	1200
...	9	12	960	600
...	8	11	470	350
...	7	10	210	190
...	6	9	85	102

a corresponding range of  $n$  values for  $K^-p$  with the same min ( $\Delta n$ ). Picking the mean  $n$  of each range, we multiply  $\Gamma_A^{Kp}$  by the scaling factor from Eq. (4.46) to obtain an average  $\Gamma_A^{\Sigma d}$  which we use over the range of  $n$  values in  $\Sigma^-d$ . The numbers involved in the calculation are collected together in Table X.

For fixed mass  $m_{ab}$  and increasing  $n$ ,  $\Gamma_A^{ab}$  eventually begins to decrease because the concomitant increase in  $\Delta n$  implies the initial and final wave functions in  $\langle n' | r | n \rangle$  differ more in radial extent and number of nodes. In fact, above  $n=28$  we expect  $\Gamma_M$ , the rate of de-excitation by molecular dissociation, to predominate over  $\Gamma_A$  on the basis of the following estimate of the former rate:

$$\Gamma_M \approx \frac{1}{2} N V_{th} \pi a_0^2 (n/38)^2 \quad (4.49)$$

(the factor  $\frac{1}{2}$  appears because  $N$  is the density of deuterium atoms).

From each  $n$  level the fraction of  $\Sigma^-$  captured will be

$$\Delta_n = f_{arr}(n) \tau_n^{-1} [\tau_n^{-1} + \Gamma_A + \Gamma_M]^{-1}, \quad (4.50)$$

$$\tau_n^{-1} = \tau_1^{-1} \tilde{f}(n)/n, \quad (4.51)$$

where  $f_{arr}(n)$  is the fraction of hyperons which arrive at the  $n$ th level. We estimate

$$f_{arr}(n) \approx 1/\min(\Delta n). \quad (4.52)$$

The fraction of  $\Sigma^-$  surviving to  $n \leq n_0$  is

$$N(n_0)/N(38) = \prod_{n>n_0}^{38} (1 - \Delta_n). \quad (4.53)$$

Table XI presents the life history of a  $\Sigma^-$  from  $n=38$  to  $n=8$ . For each  $n$  range in  $\Sigma^-d$  a value for  $\tau_n^{-1}$  was obtained from Table VI or VII by means of linear interpolation where required. From Eqs. (4.42) and

TABLE XI. Capture schedule for  $\Sigma^-$  hyperons.  $(1-\Delta)$  gives the probability  $N(n_0-1)/N(n_0)$  that a  $\Sigma^-$  in  $n=n_0$  will survive to  $n < n_0$ , calculated for the mean value in the  $n$  range of column 1, and  $p$  is the number of levels in this range. Rates are in units of  $10^{10}$  sec $^{-1}$ . Values of  $\min(\Delta n)$  in parentheses are calculated from the energy of molecular dissociation.

$n$ range	$\min(\Delta n)$	$\Gamma_M$	$\Gamma_A^{\Sigma p}$	$n^3 \Gamma = 3 \times 10^{17}$ sec $^{-1}$		$n^3 \Gamma = 1 \times 10^{18}$ sec $^{-1}$	
				$\tau_n^{-1}$	$(1-\Delta)^p$	$\tau_n^{-1}$	$(1-\Delta)^p$
38	(6)	16		0.5	0.97	1.6	0.91
32	(4)	11		1.0	0.92	3.7	0.83
28-27	(3)	8.4	8.5	2.1	0.93	5.4	0.80
26-24	5		21	3.0	0.91	6.5	0.87
23-22	4		29	4.5	0.93	9.5	0.88
21-19	3		35	6.9	0.89	11	0.84
18-15	2		150	10	0.88	16	0.82
14-13	1		1200	18	0.98	14	0.98
12			600	19	0.97	13	0.98
11			350	18	0.95	12	0.97
10			190	18	0.91	10	0.95
9			102	17	0.86	8.0	0.93
			$N(26)/N(38)$		0.83		0.55
			$N(8)/N(26)$		0.47		0.43
			$N(8)/N(38)$		0.39		0.24

(4.44), and the results of the table, it follows that  $\Delta r_b/r_b \approx 10\%$ .

## V. CONCLUSION

In cases such as global symmetry, in which one or more of the two-body scattering lengths are large, one can list three assumptions of the present calculation which might be poorly satisfied, so that the calculated  $r_b$  would not be accurate. We discuss at any length only uncertainties springing from the present calculation. The uncertainties in the calculation of reference 6 concern mainly the treatment of the short-range forces, which there are approximated by a hard core in the potential.

### A.

The corrections for the  $\Sigma-\Sigma^0$  mass difference were carried out as though the forces were zero range. The corrections to  $A^{-1}$ , the inverse scattering length matrix, which most probably are of order  $\frac{1}{2}R(2m\Delta M)$ , would be appreciable for large  $A$ . In fact, the effective range corrections of de Swart and Dullemond, which are of this order, change the sign of the  ${}^1S_0$ ,  $I=3/2$   $A$ -matrix element: from  $A_{3/2} = +22$  F to  $A_{3/2} \approx -20$  F.<sup>6</sup> That is, after the  $A$  matrix is transformed from basis states of definite isospin to basis states of definite charge and corrected for finite range effects, the  $A$  matrix appears as though it had been calculated directly from an  $A$  matrix in isospace with a large negative  $A_{3/2}$ .

This change does not greatly affect either  $T$  or  $r_b$  [when a single scattering length is large, it dominates both the numerator and denominator of Eq. (3.3) for  $T$ , and its precise magnitude and phase tend to cancel out in taking the ratio]; however, taken in conjunction with effects  $B$  and  $C$  to follow, the mass-splitting correction could lower  $r_b$  appreciably.

We note that  $A_{3/2}$  is required to be negative if it is large, since a large positive value would imply a  $\Sigma^-n$  bound state which has not been observed.

A large  $A_{3/2}$  is characteristic of global symmetry solutions, since this hypothesis relates  ${}^1S_0$ ,  $I=3/2$ ,  $\Sigma N \rightarrow \Sigma N$  scattering to  ${}^1S_0$ ,  $I=0$ ,  $NN \rightarrow NN$  scattering, which is quite strong at low energies.

### B.

The two-body amplitude was approximated by its value at the most probable momentum. However, the spectator particle carries off a varying amount of the momentum from the site of the  $YN$  interaction.

In the  $\Lambda$  channel the effects of this momentum variation should be small for small scattering lengths even though the kinematics allow a large spread in  $q_s'$ ,  $0 \leq q_s' \leq 1.6$  F $^{-1}$ . The  $q_s'$  momentum distribution

$$|\langle q | d \rangle|^2 \times \text{phase space} \approx [\alpha^2 + q_s'^2]^{-2} q_s'^2 (2m_{n(\Lambda n)} Q_\Lambda - q_s'^2)^{1/2} \quad (5.1)$$

is sharply peaked at  $q_s' \approx \alpha \pm \alpha = 0.23 \text{ F}^{-1} \pm 0.23 \text{ F}^{-1}$  (the limits give the half-maxima). The corresponding values of  $p_{\Sigma p}$  and  $q_{\Lambda n'}$ , from Eqs. (3.6) and (3.7), are  $0.1 \pm 0.1$  and  $1.40 \pm 0.2 \text{ F}^{-1}$ , respectively. For comparison, in Sec. II the  $T$  matrix was approximated by its value at  $p_{\Sigma p} = 0$ ,  $q_{\Lambda n'} = 1.42 \text{ F}^{-1}$ .

In the  $\Sigma^0$  case the amplitude which leads to the dominant term in the rate is that to the  $nn \ ^1S_0$  state. For this final state the integration (2.4) over virtual spectator momenta  $p_s' \neq q_s'$  is nonvanishing. One can estimate the average  $p_s'$  by inspection of the several factors in the integrand (approximated by their leading terms),

$$\int_{-\infty}^{+\infty} \frac{T(p_s')}{p_{nn}{}^2 - q_{nn}{}^2 \alpha^2 + p_s'^2} d^{(3)}p_s' \quad (5.2)$$

Very roughly,  $p_s'^2 (p_{nn}{}^2 - q_{nn}{}^2)^{-1} \approx 1$  for large enough  $p_s'$  [see Eq. (3.9)], so that eventually the integral goes as

$$\int_0^{\infty} \frac{T(p_s')}{\alpha^2 + p_s'^2} d^3p_s' + i\pi q_{nn} \int \frac{T}{\alpha^2 + p_s'^2} d\Omega_{nn}. \quad (5.3)$$

The second term comes from the pole at  $p_{nn}' = q_{nn}'$ . In this term,  $T$  becomes averaged over values of  $p_s'$  lying in the physical range,  $0 \leq p_s' \leq 0.18 \text{ F}^{-1}$ . However, in the first term there are important contributions to the integrand from values of  $p_s'$  of order  $\alpha$ .

We estimate the effects of spectator recoil by adding an effective range term  $\frac{1}{2}R_{3/2}(p_{\Sigma n})^2$  to  $-A_{3/2}^{-1}$ . Choosing  $R_{3/2} = 3 \text{ F}$  (the value given by reference 6), and  $p_s' \approx 2\alpha$ , so that from Eq. (3.8)  $p_{\Sigma n} \approx \alpha$ , we get  $\frac{1}{2}R_{3/2}p_{\Sigma n}^2 \approx 0.08$ . Since  $-A_{3/2}^{-1} \approx 0.05$  after the mass difference effects of part A above were taken into account, we find  $A_{3/2}$  roughly halved in magnitude to  $A_{3/2} \approx -8 \text{ F}$ .

This value is still too large to bring one within the experimental upper limit on  $r_b$ . If one were to repeat the calculation of  $r_b$  with smaller  $A_{3/2}$  but with all other  $A$ -matrix elements kept as before, one would reach the experimental upper limit at  $A_{3/2} \approx -1 \text{ F}$  (or  $+5 \text{ F}$  in the positive direction) and the mean experimental value for any  $A_{3/2}$  in the range  $A_{3/2} \approx -0.5$  to  $+1 \text{ F}$ . The experimental  $r_b$  is quite consistent with  $\Lambda$  and  $\Sigma^0$  scattering parameters comparable in magnitude.

### C.

Multiple scattering effects were not taken into account in computing the amplitude by impulse approximation. In order for multiple scattering to affect  $r_b$  strongly, two conditions must be satisfied.<sup>20</sup>

(i)  $\exp(ip_{\Sigma n}R)\langle\Sigma^0|T|\Sigma^-\rangle/R$  must be of order unity.  $R$  is a typical internuclear distance in the deuteron. We can neglect contributions  $\exp(ip_{\Lambda n}R)\langle\Lambda|T|\Sigma^-\rangle/R$  from rescattered  $\Lambda$  particles, even were  $\langle\Lambda|T|\Sigma^-\rangle$  large: On integration over  $R$ , contributions from different  $R$  largely cancel one another due to the rapid oscillation of  $\exp(ip_{\Lambda n}R)$ . Contributions from rescattered  $\Sigma^-$  do not

TABLE XII.  $T$ -matrix elements (in F) for estimation of multiple scattering effects; from global symmetry results for the  $^1S_0$  channel. The  $\Sigma^-\Sigma^0$  mass difference is taken into account according to the method of Sec. II.

$\langle\Lambda n T \Sigma^-\rangle$	$-0.072i - 0.24$
$\langle\Lambda n T \Sigma^0 n\rangle$	$-0.042i + 0.026$
$\langle\Sigma^0 n T \Sigma^-\rangle$	$3.47i - 1.47$
$\langle\Sigma^0 n T \Sigma^0 n\rangle$	$5.34i - 2.22$

affect  $r_b$  since final  $\Lambda$  and  $\Sigma^0$  channels will be enhanced proportionate to their values in the impulse approximation limit, and the multiple scattering effect drops out in computing the ratio  $r_b$ . Condition (i) is certainly met in the global symmetry case.

(ii) The returning  $\Sigma^0$  must interfere constructively with production of one hyperon, and destructively with production of the other; or at least its effect must be appreciably different in the two channels. Otherwise the effect will again drop out on computing the ratios  $r_b$  and  $r_f$ .

In the global symmetry case, the amplitude  $\langle Y^0 n|T|\Sigma^0 n\rangle$  for production by the returning  $\Sigma^0$  interferes constructively with the  $\langle Y^0 n|T|\Sigma^-\rangle$  amplitude in both final channels (Table XII), so that the effect  $C$  may not be too important in this particular case.

An interesting conceivable source of extreme three-body effects would be a  $\Sigma NN \ T=1$  metastable bound state. A discussion using impulse approximation would not be relevant if such a hyperfragment existed, although some remarks on observable consequences are appropriate. The most probable mode of formation for the conjectured hyperfragment would be by electric dipole transition from an  $l=1$  Bohr orbit. (We are assuming all internal angular momenta of the final state to be  $l=0$ .) For a photon of energy  $\omega$ , the rate goes as  $|\langle r \rangle|^2 \omega^3$ , where  $\langle r \rangle$  is a typical nuclear dimension, probably at least a factor 10 down from the Bohr radius of the  $\Sigma^-d$  system ( $37 \text{ F}$ ). Therefore, in order to compete even with radiative  $nP \rightarrow 1s$  transitions, the binding energy should be such as to give rise to a photon of energy at least of order  $\omega \approx 10^{2/3} \omega_R = 4.6 \omega_R$ , where  $\omega_R$ , the Rydberg energy, is  $19 \text{ keV}$  for  $\Sigma^-d$ . It is likely that  $\Sigma^-d$  will be weakly bound if it exists at all, however, especially in view of the fact that the lighter hyperfragment  $\Sigma n$  has not been found. Therefore, it would be entirely reasonable to expect few transitions to this hyperfragment and consequently no great effect, arising from its subsequent decay via strong interactions, on the spectrum of final  $\Lambda$  particles. This conclusion might hold even in the case of a moderately large branching ratio, since the momentum spectrum of  $\Lambda$ 's from the hyperfragment could be very similar to that of the  $\Lambda$ 's directly from Bohr orbits, if the momentum distribution of the nucleons in the hyperfragment were still deuteron-like. (The end point of the spectrum would, of course, be somewhat lower.) Thus, if such a metastable state existed, it would probably not show up until such time as

<sup>20</sup> L. H. Schick, Rev. Mod. Phys. 33, 608 (1961).

TABLE XIII. Effect of  $\Gamma_M \rightarrow G\Gamma_M$  on depletion of  $\Sigma^-$  hyperons during cascade.

G	N(26)/N(38)		N(8)/N(38)		$\Delta r_b/r_b$
	$n^3\Gamma = 3 \times 10^{17} \text{ sec}^{-1}$	$n^3\Gamma = 1 \times 10^{18} \text{ sec}^{-1}$	$n^3\Gamma = 3 \times 10^{17} \text{ sec}^{-1}$	$n^3\Gamma = 1 \times 10^{18} \text{ sec}^{-1}$	
5	0.95	0.84	0.44	0.36	0.05
1	0.83	0.55	0.39	0.24	0.10
1/2	0.73	0.43	0.36	0.18	0.12
1/4	0.59	0.24	0.28	0.10	0.12

the  $\gamma$  spectrum of this process became available for study.

Effects *A* and *B* together have brought  $A_{3/2}$  from +22 F to  $\approx -8$  F. Our estimates were crude, and it is entirely possible that more accurate ones would reduce  $A_{3/2}$  still further. However, it seems unlikely that these effects would reduce  $A_{3/2}$  as far as the values  $A_{3/2} \gtrsim -1$  F which fit the experimental  $r_b$ .

It is heartening to note that the observed ratio can be well fitted using small scattering lengths, for which effects *A*, *B*, and *C* above are not expected to be important.<sup>21</sup>

$r_b$  is affected not only by a possible large nuclear scattering length, but also by electromagnetic spin-orbit couplings which cause transitions between initial states of different total spin. For captures from  $n > 8$ , these couplings are so weak that formula (2.34) is an excellent approximation to  $r_b$ . For captures from  $n \leq 8$  uncertainty in estimating the effect of spin-state mixing stems from the uncertainty in estimating the depletion of  $\Sigma^-$  during cascade down to  $n \leq 8$ . We discuss three sources of uncertainty.

### 1. The Estimate of $\sigma_m$

If the cross section for de-excitation via molecular dissociation were reduced by a factor *G* from the geometrical assumed in Sec. 4,

$$\sigma_M \rightarrow G\pi a_0^2 (n/38)^2 \quad (5.4)$$

$\Delta r_b/r_b$  should increase. Decreasing *G* increases the time spent in  $n \geq 28$ , where quartet and doublet states differ greatly in their values of  $\tau^{-1}$ . Consequently the spin distribution becomes shifted farther from statistical. Table XIII shows, however, that the effect is small.

Further, unlimited reduction in *G* does not lead to unlimited error in  $r_b$ ; for  $G \lesssim 1/2$  even the more slowly captured state will become seriously depleted while in  $n \geq 28$ .

### 2. The Estimate of $V_{th}$

As the subscript indicates, we have simply taken the thermal value for the  $\Sigma^-d$  translational velocity. Bethe

<sup>21</sup> de Swart and Iddings, who calculate *YN* scattering from meson-theoretic potentials with hard cores, find such small scattering lengths for a wide range of  $\Sigma\Sigma\pi$  and  $\Lambda\Sigma\pi$  coupling constants and reasonable values of core radii  $x_0$ . They obtain values of  $r_b < 0.6$  for  $-0.05 \lesssim f_{\Sigma\Sigma} \lesssim +0.1$  and  $0.25 \lesssim f_{\Lambda\Sigma} \lesssim 0.35$ , with  $0.3 \lesssim x_0 \lesssim 0.4$  (in units of pion Compton wavelength). These values include unitary symmetry ( $f_{\Sigma\Sigma} = 0, f_{\Sigma\Lambda} = 0.28$ ) but not global symmetry ( $f_{\Sigma\Sigma} = f_{\Lambda\Sigma} = 0.29$ ).

and Leon, however, use a velocity about five times thermal, arguing that the immediate past history of the  $\Sigma^-d$  atom is one of de-excitation via molecular dissociation, from which the  $\Sigma^-d$  atom should emerge with about 1 eV translational energy. Since  $\Gamma_M \propto V\sigma_M$ , while  $\Gamma_A$  is independent of *V* for all *n* and  $\tau_n^{-1}$  is roughly independent of *V* for  $n \gtrsim 28$  [because approximation (4.25) for  $\hat{f}(n)$  holds for these *n*], taking  $V \rightarrow 5V$  has the same effect on depletion from  $n \gtrsim 28$  as taking  $G = 5$  in Eq. (5.4). The depletion for  $G = 5$  is given in Table XIII. If now we examine low *n*,  $28 > n > 8$ , we find depletion will increase as *V* increases;  $\tau_n^{-1} \propto V\hat{f}(n)$  goes over to linear dependence on *V* as  $\hat{f}(n) \rightarrow 1$ . Therefore, in both *n* ranges, the increase in *V* should bring about a decrease in  $\Delta r_b/r_b$ . If we approximate the change in depletion from  $28 > n > 8$  by the change in depletion from  $n = 9$ , where  $V \rightarrow 5V$  produces the greatest effect, we get  $N(8)/N(26) \lesssim 0.33$  for both  $\Gamma$  and, therefore,  $\Delta r_b/r_b \lesssim 0.02$ . We have not taken into account the effects of the increase in  $V_\theta$  with *V*. Increasing  $V_\theta$  slows but does not reverse the trend towards more depletion from low *n*, so that we still expect a decrease in  $\Delta r_b/r_b$ . Further, we have not taken into account that, when  $V \rightarrow 5V$ , spin mixing may be neglected for an additional level,  $n = 8$ . Thus, our previous estimates for  $\Delta r_b/r_b$  may have been too high, especially since it is difficult to imagine a mechanism which would lower *V* from  $V_{th}$ .

### 3. Estimate of $\Gamma_A$

Bethe and Leon note for  $K^-p$  that Auger rates near  $n = 11$  exceed the geometric value  $NV\pi a_0^2$  by as much as a factor of 10, and suggest that a treatment more accurate than Born approximation would reduce  $\Gamma_A^{Kp}$  in this region. Likewise in  $\Sigma^-d$  near  $n = 14$ ,  $\Gamma_A^{\Sigma d}$  exceeds geometrical even when  $V = 5V_{th}$  ( $5NV_{th}\pi a_0^2 \approx 160 \times 10^{10} \text{ sec}^{-1}$ ). If  $\Gamma_A^{\Sigma d}$  were reduced in this region, there would be greater depletion from the spin states which underwent less depletion in  $38 \geq n \geq 28$ , so that  $\Delta r_b/r_b$  would decrease.

In summary of our efforts to estimate  $\Delta r_b/r_b$ , then, it is impossible to calculate exactly the effects of spin mixing on  $r_b$ , but, however, we have estimated it;  $\Delta r_b/r_b$  appears small enough that comparison between the experimental and theoretical numbers is still possible.

If the  $\Sigma^-d$  reaction were observed in a diffusion chamber, so that the density *N* were reduced considerably, then complete equilibration of spin states

would occur between each collision. The branching ratio for capture from  $38 \geq n \geq 8$  would lie between  $r_f$  and  $r_b$ , while for capture from  $n \leq 8$  the appropriate branching ratio would be  $r_b$ .

**ACKNOWLEDGMENTS**

The author wishes to express his gratitude to Professor R. H. Dalitz, who suggested this problem, for his encouragement, suggestions, and critical discussions. It has been a great pleasure to have been associated with Dr. J. J. de Swart and Dr. C. K. Iddings during the concluding portions of this work. The author is indebted to Dr. Melvin Leon for furnishing his results in advance of publication.

**APPENDIX CAPTURE IN HYDROGEN**

For convenience, we list some formulas and results for  $\Sigma^-$  capture by the free proton.

$$\begin{aligned} \Gamma_{S^Y} &= \pi^{-1} |\psi_{ns}(0)|^2 m_Y n [2m_Y n Q_Y(H)]^{1/2} |A_{S^Y}|^2, \\ \Gamma_{T^Y} &= \pi^{-1} |\psi_{ns}(0)|^2 m_Y n [2m_Y n Q_Y(H)]^{1/2} |A_{T^Y}|^2 \\ &\quad + [2m_Y n Q_Y(H)]^2 |D^Y|^2. \end{aligned} \tag{A1}$$

$$\begin{aligned} \Gamma_S &\approx (1.19 \times 10^{18}/n^3) |\Lambda_S|^2 \text{ sec}^{-1}, \\ \Gamma_T &\approx (1.19 \times 10^{18}/n^3) |\Lambda_T|^2 + 4.33 |\Lambda_{TD}|^2 \text{ sec}^{-1}. \end{aligned} \tag{A2}$$

Contributions from  $|\Sigma_{S,T}|^2$  terms are down by a factor

of  $[Q_\Sigma(H)/Q_\Lambda(H)]^{1/2} = [3.1/79.3]^{1/2} \approx 1/5$ . Taking  $|\Lambda|^2 = 0.1 \text{ F}^2$ , we get

$$\begin{aligned} \Gamma_S &\approx 1 \times 10^{17}/n^3, \\ \Gamma_T &\approx 5 \times 10^{17}/n^3. \end{aligned} \tag{A3}$$

In Table XIV are given the results of a calculation of

TABLE XIV. Depletion from  $\Sigma^-p$ .

$n^3\Gamma$	$1 \times 10^{17}$	$5 \times 10^{17}$
$N(23)/N(33)$	0.81	0.48
$N(6)/N(23)$	0.39	0.37
$N(6)/N(33)$	0.32	0.18

depletion from  $\Sigma^-p$ , for  $V = V_{th}$  and  $G = 1$ . Using

$$\delta(H) = \frac{3}{4} [N_S(6)/N_S(33) - N(6)/N(33)], \tag{A4}$$

$$\begin{aligned} \Delta r_b(H)/r_b(H) &= \frac{1}{4} \delta(H) \left[ -\frac{\Gamma_S^\Sigma}{\Gamma_S} + \frac{\Gamma_T^\Sigma}{\Gamma_T} \right] / \\ &\quad \left[ \frac{1}{4} \frac{\Gamma_S^\Sigma}{\Gamma_S} + \frac{3}{4} \frac{\Gamma_T^\Sigma}{\Gamma_T} \right], \end{aligned} \tag{A5}$$

$$|\Delta r_b(H)/r_b(H)| < |\delta(H)|, \tag{A6}$$

we get

$$|\Delta r_b(H)/r_b(H)| < 11\%.$$